

# Novel Approach for the Bonding of III-V on Silicon Tandem Solar Cells with a Transparent Conductive Adhesive

Ulrike Heitmann, Sven Kluska, Jonas Bartsch, Hubert Hauser, Alexey Ivanov, Stefan Janz

Fraunhofer Institute for Solar Energy Systems ISE, Heidenhofstraße 2, 79110 Freiburg, Germany

**Abstract** — The currently used options for the monolithic interconnection of sub-cells in a Si and III-V tandem solar cell device are direct wafer-bonding or hetero-epitaxy. Both methods are costly and difficult to transfer into an industrial process. This work presents a novel, scalable and cost-efficient process for the interconnection of semiconductor substrates by using a transparent conductive oxide (TCO) interlayer. The TCO material is sprayed from a solution onto both sub-cells which are subsequently connected by using a hot press. The resulting bond shows optical absorption below 2% and a connecting resistivity of  $2 \Omega\text{cm}^2$ . Bonded samples withstood all further processing steps and thereby demonstrated mechanical stability of the bond.

## I. INTRODUCTION

One promising way to increase the efficiency of a non-concentrator single junction solar cell is combining semiconductor absorber materials with different bandgaps into a tandem solar cell in order to decrease the thermalization losses. The most used techniques for combining the sub-cells are direct growth [1], direct wafer bonding [2] and mechanical stacking [3]. The hetero-epitaxial growth and the direct wafer bonding both require extensive surface preparation which makes them costly and difficult to scale into an industrial process. The mechanical stacking involves a non-conductive interlayer leading to a four terminal device, which has to deal with lateral conductivity and the implementation in existing PV module concepts.

One possible solution for an industrially feasible interconnection of tandem solar cells is to apply a transparent conductive adhesive (TCA). The main challenge in the realization of TCAs is to find an optimum between conductivity and transparency as most TCAs obtain electrical conductivity by the addition of non-transparent, conductive metal particles [4].

A material that could circumvent the trade-off between transparency and conductivity of common TCAs are transparent conductive oxides (TCO). Common representatives of TCOs like Indium Tin Oxide (ITO) and Aluminum or Indium doped Zinc Oxide (AZO/IZO) are well known and widely deployed in display technology [5].

In the field of solar cell technology, TCOs are mainly applied in heterojunction devices [6]. In the field of tandem solar cells with III-V and Si absorbers, only one reference reports the application of Indium Zinc Oxide thin films as a protective coating during the wafer bonding process [7]. In this publication we present for the first time a process using

spray-coated TCO which is used for the mechanical, optical and electrical interconnection of two semiconductor substrates.

## II. EXPERIMENTAL

In order to enable the utilization of the TCO material for the bonding of a tandem solar cell, a process similar to that of the sol-gel synthesis of TCO thin films [8] is applied. To ensure a good contact of the TCO material to the semiconductor substrate, an initial TCO layer is deposited by spray pyrolysis [9]. Both processes involve the same precursor solution, containing the TCO compounds dissolved in an organic solvent. The processes differ in the substrate temperature: while the spray pyrolysis is carried out at substrate temperatures  $>300^\circ\text{C}$ , the substrate temperature during the deposition of the sol-gel like adhesive layer is set to  $100^\circ\text{C}$ . In contrast to the sol-gel processed bond-layer, the TCO layer deposited by spray pyrolysis exhibits an oriented, polycrystalline structure. On top of the polycrystalline TCO layer, a sol-gel like layer of the same TCO is sprayed. The sol-gel layer is adhesive, allowing a first bonding of the two semiconductor substrates. In order to anneal the sol-gel layer and thereby provide the electrical interconnection of the two substrates, the sample is placed in a hot press. Fig. 1 shows a sketch of the developed process flow.

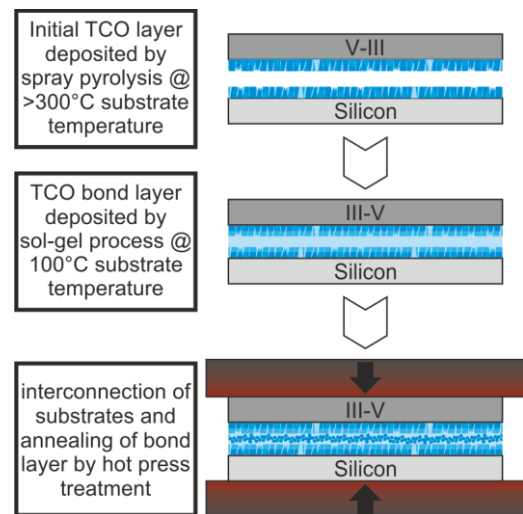


Fig. 1. Sketch of the developed process flow for the mechanical, optical and electrical bonding of a III-V/Si tandem solar cell using sprayed TCO layers.

### III RESULTS

The electrical and optical characterization was carried out on bonded silicon substrates and bonded glass substrates, respectively. Since this work is focused on developing a TCA for silicon based tandem solar cells, silicon was chosen as semiconductor material.

#### A. Optical Characterization

The transparency of the used TCO material was investigated along the process route: first after spraying the initial, polycrystalline layer and second after the hot press treatment. The TCO material was sprayed onto 0.7 mm Schott Borofloat glass substrates. The absorption of a single TCO layer on glass and the absorption of bonded glass substrates measured with a PerkinElmer Lambda950 UV-Vis Spectrometer are shown in Fig. 2. The edge in the absorption spectra around 860 nm is an artefact related to a change of detector within the UV-Vis spectrometer. In the relevant wavelength range from 600 to 1100 nm the absorption is  $\leq 2\%$ .

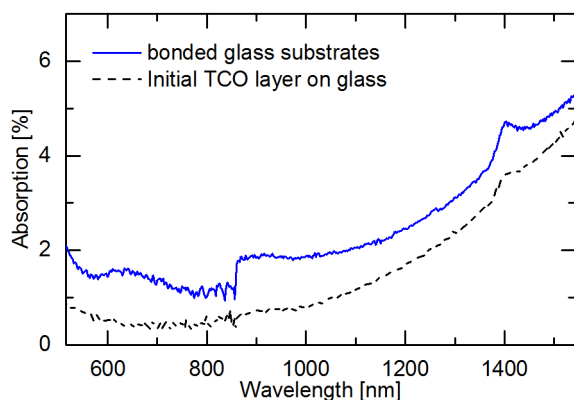


Fig. 2. Absorption of the initial TCO layer (thickness  $\approx 100$  nm) deposited on 0.7 mm Borofloat glass substrates and absorption of two 0.7 mm glass substrates bonded with the developed adhesive.

#### B. Bond quality

The homogeneity and appearance of the bond layer in between the silicon substrates was analyzed by Scanning Acoustic Microscopy (SAM, PVA TePla WINSAM 8 equipped with a 30 MHz transducer) and Scanning Electron Microscopy (SEM, Zeiss Auriga 60). The used sample structure consisted of 4" n-type, 1  $\Omega$ cm FZ silicon substrates with a shiny etched surface. An n-type emitter was diffused into both sides, creating a symmetric  $n^{++}/n/n^{++}$  sample structure. Prior to the spray pyrolysis process, the surface was treated with 1% hydrofluoric acid (HF) for 30 s. The bonding of the two substrates was carried out according to Fig. 1.

The SAM scans the sample in various depths of the sample and superimposes the scans to generate an image of the bond layer. In Fig. 3 the first scan of the sample's surface (right) and a scan of the bond layer (left) are shown. By comparing the

two scans it can be found, that the small dark spots correspond to surface contaminations (top right) while the dark area within the center most likely represents the bonded area.

A SEM cross section was prepared in the position indicated by a star in Fig. 3. It shows both the initial sprayed TCO layer and the adhesive, sol-gel like TCO layer. The initial TCO layer, deposited by spray pyrolysis, shows a homogeneous, polycrystalline structure with a constant thickness of  $\approx 100$  nm (Fig. 3, bottom left). The annealed adhesive layer shows voids, which are presumably caused by the evaporation of organic compounds of the sol-gel like bond layer during the hot-press treatment (Fig. 3, bottom right). Within these voids of the annealed adhesive layer, larger formed structures indicate the partial crystallization of the adhesive TCO layer. The recrystallization of the sol-gel like bond layer should make the bond electrically conductive.

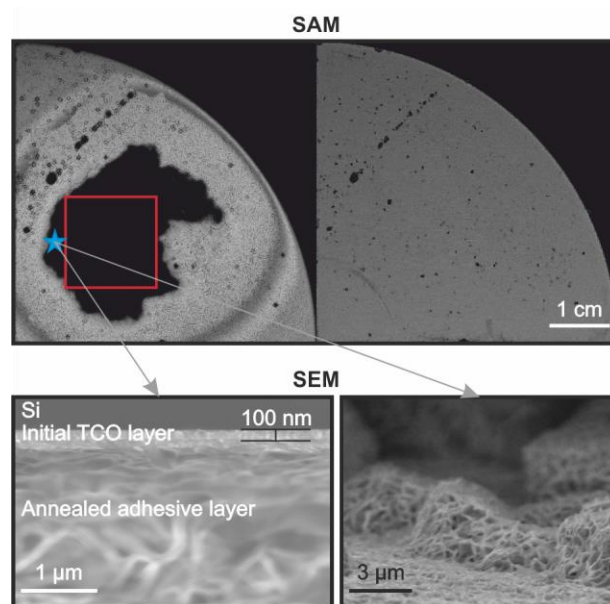


Fig. 3. Top: SAM mapping of the bonded interface (left) and only the sample's surface (right). The red square indicates the area cut out for the electrical characterization. Bottom: SEM cross-section in the indicated position (left) and tilted top-view of the structure of the annealed adhesive layer within a void (right).

In order to obtain a fully bonded sample, a second set of experiments was carried out. This time, the substrates were standard 4" FZ silicon with a shiny etched surface on both sides but without a diffused emitter. The bonding process was carried out according to the process sketch in Fig. 1. The only variation in this experiment was the spraying of the sol-gel like adhesive layer, which was repeated multiple times from 7 up to 20 times. It was expected that a thicker sprayed adhesive layer generates a larger bonded area, since it would be less sensitive to particles on the substrates surface.

The bonded samples were characterized by Scanning Acoustic Microscopy and the resulting images are shown in

Fig. 4. Each scan shows the superimposed image of all scans at various depths within the sample.

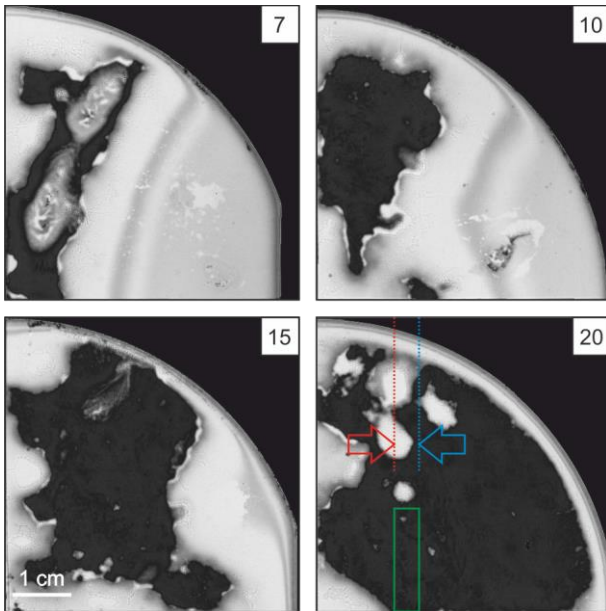


Fig. 4. SAM scans of bonded Si samples with increasing number of spraying iterations for the sol-gel like adhesive layer (from 7 times, upper left to 20 times, lower right scan). The dark area corresponds to bonded areas while the white area corresponds to voids in between the two substrates.

The SAM scans show an increase of the bonded area with an increasing number of spray iterations. By further increasing the number of iterations a complete bonding of the two substrates should be possible according to this study.

In order to investigate the adhesive layer for its porosity and overall structure, the sample with 20 spray iterations was prepared for cross-section analysis and mechanical testing. In Fig. 4 the red (left) and blue (right) arrows indicate two cross sections prepared for SEM analysis which can be found in Fig.5. The green square indicates the slice that has been cut for mechanical testing.

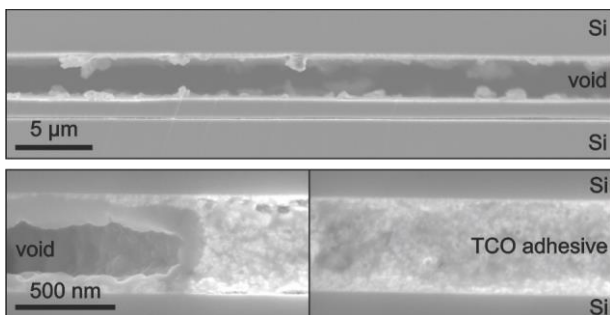


Fig. 5. SEM analysis of the two prepared cross-sections. The upper cross-section corresponds to the area indicated by the red arrow in the SAM scan and the lower two cross-sections correspond to the area indicated by the blue arrow.

In Fig. 4 the red arrow points to an area which is presumably not bonded while the blue arrow points to an area selected for its apparently complete bond. The SEM analysis of these two areas confirms the SAM based assumptions. In Fig. 5 the upper cross sections shows a void in between the upper and lower silicon substrate of approximately 3 μm width. The lower two cross sections were prepared in an area that appeared black in the SAM scan (Fig. 4, blue arrow). Both show a distance between the two silicon substrates of ≈500 nm and most of the bond is filled with the adhesive layer (Fig. 5, lower right cross section). The adhesive layer is not completely homogeneous within this cross section but shows some void as can be found in the lower left cross section in Fig. 5.

### C. Mechanical properties

The mechanical strength of the bond was tested with the Maszara blade test, where a thin blade is inserted in between the two substrates and the formed fissure is analyzed. In Fig. 4 the area that was cut out for mechanical testing is shown (green square). In Fig. 6 an infrared transmission picture is shown (1) before, (2) while and (3) after inserting the 140 μm thin blade in between the two silicon substrates.

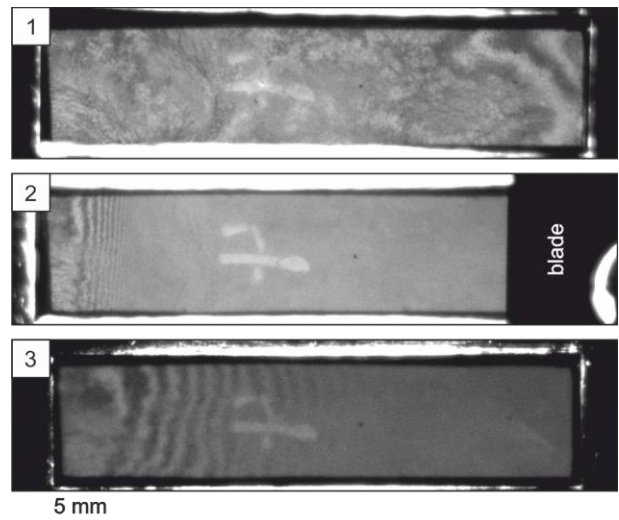


Fig. 6. IR transmission pictures of a bonded sample. Top: sample before inserting the blade. Middle: sample with the blade inserted. Bottom: Sample after removing the blade.

The IR pictures show, that inserting the blade leads to an opening of a fissure of approximately 15 mm length. At the left side of the sample, a 2 mm wide area remains bonded. Comparing the thickness of the blade (140 μm) with the thickness of the adhesive layer (≈500 nm), this results can be interpreted as a rather good bond strength. More importantly, all samples withstood process steps like sawing and ion-polishing, which also indicates good mechanical bond strength.

#### D. Electrical Characterization

When considering the structure of the bonded sample, it can be stated that the electrical resistance of the bond interface mainly originates from the contact resistance of the TCO/semiconductor interface and the resistivity of the annealed adhesive layer (see Fig. 7). The contact resistance of the initial, polycrystalline TCO thin film to a highly doped silicon surface was measured by the transfer line method (using evaporated Ti/Pd/Ag metal pads) and ranged between  $0.3 - 1 \Omega \text{ cm}^2$ . The resistivity of the annealed adhesive layer was indirectly analyzed by measuring the dark I-V curve of the whole bonded sample. Again a Ti/Pd/Ag metal layer was deposited on both sides of the bonded sample. For better comparison of results, a fully bonded  $1.5 \times 1.5 \text{ cm}^2$  square was cut from the sample. The position of the square was chosen according to the SAM scan in Fig. 3. A schematic of the cross-section of the bonded sample as well as the measured I-V curve are shown in Fig. 7.

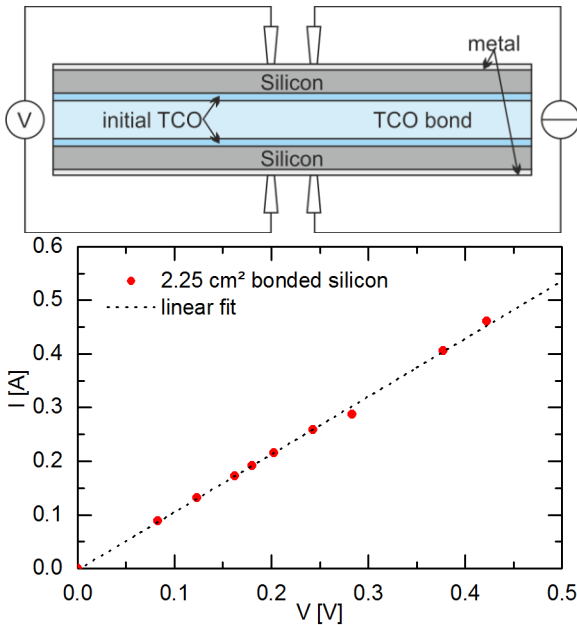


Fig. 7. Top: Sample structure for I-V measurement. Bottom: Measured I-V curve of bonded sample.

The I-V curve shows an ohmic behavior of the bonded stack and a resistance of  $1.1 \Omega$ . Compared to the total resistance of the bonded sample, the contact resistance of the Ti/Pd/Ag metallization on the front and rear side of the sample should be negligible. The resistance of the two silicon substrates amounts to  $0.2 \Omega$ . This results in a resistance of  $0.9 \Omega$  for the sol-gel like adhesive layer. By multiplying with the area of the sample, a connecting resistivity of  $2 \Omega \text{ cm}^2$  can be calculated. According to *Yoshidomi et al.* [10], this connecting resistivity is low enough to limit the bond related efficiency losses to just  $\approx 1 \%$  abs., when assuming a  $V_{OC}$  of  $3.1 \text{ V}$ , which has been demonstrated for comparable structures of Si-based multi-

junction solar cells [11]. As the technology is currently in an early development stage, it is expected that this loss can be further reduced upon process optimization. Also, some loss compared to direct wafer bonding is acceptable if the costs can be lowered disproportionately, which is expected for the cost-efficient spray coating solution used in the presented approach.

In a final device, the developed transparent conductive adhesive has to electrically contact not only the silicon substrate but also the III-V material of the top cell. In order to investigate the electrical contact of the TCO and the III-V top cell, test structures consisting of a p-type GaAs substrate with an epitaxial  $p^{++}$  contact layer on the surface were prepared. The epitaxial layer was then coated with the initial TCO layer (according to the process sketch in Fig. 1) and metal contacts were deposited onto the TCO and the rear side of the GaAs substrate. A sketch of the test structures is shown in Fig. 8.

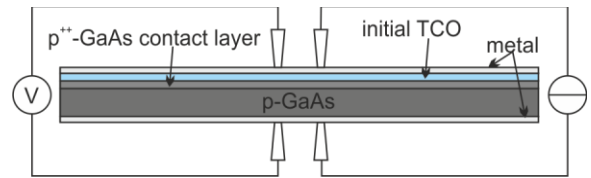


Fig. 8. Test structure used to investigate the electrical contact of the sprayed TCO layer to the epitaxial  $p^{++}$  GaAs contact layer.

After cutting the sample into  $5 \times 5 \text{ mm}^2$  squares the I-V characteristics of the samples were analyzed. In Fig. 9 an exemplary I-V curve for one of the  $25 \text{ mm}^2$  samples is shown.

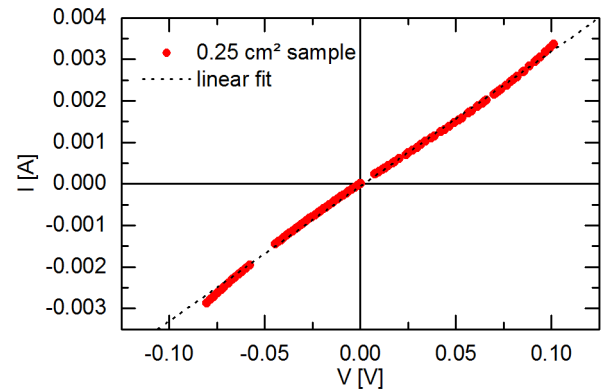


Fig. 9. I-V curve of a  $25 \text{ mm}^2$  p-GaAs sample sprayed with the initial TCO layer on top of an epitaxial  $p^{++}$ -GaAs contact layer.

The curve shows almost ohmic behavior, which indicates, that the n-type, initial TCO layer is capable of forming an ohmic contact to the  $p^{++}$  GaAs layer. The high resistance of  $30.8 \Omega$  could originate from the fact that prior to spraying the TCO layer no cleaning of the epitaxial surface was performed. Further analysis of this TCO – III-V contact will be carried out. However, in this early stage of development the fact that

the spray coated TCO forms an ohmic contact to both semiconductors ( $n^{++}$  Si and  $p^{++}$  GaAs) is an exciting result.

#### IV. SUMMARY

The presented work shows a new and scalable approach for the mechanical and electrical bonding of semiconductors. In contrast to existing methods, the transparent conductive adhesive material used does not contain any conductive, non-transparent particles. By combining the techniques of spray pyrolysis and sol-gel deposition, a simple process was developed, where the precursor solutions are sprayed onto the heated substrates. The resulting bond shows absorption of less than 2% in the relevant wavelength range and a connecting resistivity of  $2 \Omega \text{cm}^2$ , which would result in an efficiency loss of  $\approx 1\%$  abs. assuming a  $V_{OC}$  of 3.1 V.

The bonded area increased with the number of spraying iterations of the adhesive layer and the mechanical strength of the bond is good enough to withstand all processing steps. The Maszara blade test shows an opened fissure of 15 mm length but the sample remained bonded on the opposite side.

By spraying the initial TCO layer onto a p-GaAs substrate, the electrical properties of the TCO/ $p^{++}$ -GaAs interface were investigated. Although the resistance of the prepared 25 mm<sup>2</sup> sample is quite large ( $30.8 \Omega$ ), the curve shows almost ohmic behavior. It is expected that the contact resistance to both semiconductor materials can be further optimized, for example by implementing a cleaning procedure of the surface prior to spraying the initial TCO layer.

Spray coating is a commonly used process in industry and therefore promises straight forward scalability and cost efficiency of the developed process.

The obtained results show a proof of concept. After further optimizations regarding process homogeneity and mechanical strength of the bond as well as investigations on the electrical contact formation and conductivity the process will be applied to solar cell devices.

#### ACKNOWLEDGEMENT

The authors would like to express their gratitude to F. Dimroth, D. Lackner, F. Feldmann, R. M. da Silva Freitas, M. Winterhalder and F. Schätzle at ISE for their support and input in many valuable discussions. This work has received funding from the European Union's Horizon 2020 research and innovation programme within the project SiTaSol under grant agreement No 727497 and from the Federal Ministry for Economic Affairs within the project SolGelPV (FKZ 0324151A).

#### REFERENCES

[1] C. L. Andre, J. A. Carlin, J. J. Boeckl, D. M. Wilt, M. A. Smith, A. J. Pitera, M. L. Lee, E. A. Fitzgerald and S. A. Ringel, "Investigations of High-Performance GaAs Solar Cells Grown

on Ge-Si<sub>1-x</sub>Ge<sub>x</sub>-Si Substrates", *IEEE Trans. Electron Devices*, vol. 52, pp. 1055-1060, 2005.

[2] R. Cariou, J. Benick, P. Beutel, N. Razek, C. Flotgen, M. Hermle, D. Lackner, S. W. Glunz, A. W. Bett, M. Wimplinger and F. Dimroth, "Monolithic Two-Terminal III-V//Si Triple-Junction Solar Cells With 30.2% Efficiency Under 1-Sun AM1.5g", *IEEE J. Photovoltaics*, vol. 7, pp. 367-373, 2017.

[3] S. Essig, C. Allebe, J. F. Geisz, M. A. Steiner, B. Paviet-Salomon, A. Descoedres, A. Tamboli, L. Barraud, S. Ward, N. Badel, V. LaSalvia, J. Levrat, M. Despeisse, C. Ballif, P. Stradins and D. L. Young, "Boosting the efficiency of III-V/Si tandem solar cells", in *43rd Photovoltaic Specialists Conference*, 2016, p. 2040.

[4] L. Li, C. Lizzul, H. Kim, I. Sacolick and J. E. Morris, "Electrical, structural and processing properties of electrically conductive adhesives", *IEEE Trans. Comp., Hybrids, Manufact. Technol.*, vol. 16, pp. 843-851, 1993.

[5] D. S. Ginley and C. Bright, "Transparent Conducting Oxides", *MRS Bull.*, vol. 25, pp. 15-18, 2000.

[6] M. Taguchi, A. Yano, S. Tohoda, K. Matsuyama, Y. Nakamura, T. Nishiwaki, K. Fujita and E. Maruyama, "24.7% Record Efficiency HIT Solar Cell on Thin Silicon Wafer", *IEEE J. Photovoltaics*, vol. 4, pp. 96-99.

[7] A. C. Tamboli, S. Essig, K. A. W. Horowitz, M. Woodhouse, M. F. A. M. van Hest, A. G. Norman, M. A. Steiner and P. Stradins, "Indium zinc oxide mediated wafer bonding for III-V/Si tandem solar cells", in *42nd Photovoltaic Specialist Conference*, 2015, p. 1.

[8] J-H. Lee and B-O. Park, "Transparent conducting ZnO:Al, In and Sn thin films deposited by the sol-gel method", *Thin Solid Films*, vol. 426, pp. 94-99.

[9] M. Lucio-Lopez, M. Luna-Arias, A. Maldonado, M. de la L. Olvera and D. Acosta, "Preparation of conducting and transparent indium-doped ZnO thin films by chemical spray", *Solar Energy Materials and Solar Cells*, vol. 90, pp. 733-741.

[10] S. Yoshidomi, J. Furukawa, M. Hasumi and T. Sameshima, "Mechanical Stacking Multi Junction Solar Cells Using Transparent Conductive Adhesive", *Energy Procedia*, vol. 60, pp. 116-122.

[11] R. Cariou, J. Benick, F. Feldmann, O. Höhn, H. Hauser, P. Beutel, N. Razek, M. Wimplinger, B. Bläsi, D. Lackner, M. Hermle, G. Siefer, S. W. Glunz, A. W. Bett and F. Dimroth, "III-V-on-silicon solar cells reaching 33% photoconversion efficiency in two-terminal configuration", *Nature Energy*, vol.3, pp. 326-333.